A Controlled ENVISAT/ERS Persistent Scatterer Experiment, Implications of Corner Reflector Monitoring

Petar Marinkovic[(1)], **Gini Ketelaar**[(1)], **Ramon Hanssen**[(1)]

[(1)] ***Delft institute for Earth Observation and Space systems (DEOS),***
Delft University of Technology,
Kluyverweg 1, 2629 HS Delft, The Netherlands
Email: P.S.Marinkovic@lr.tudelft.nl

ABSTRACT

A persistent scatterer experiment using corner reflectors has been set up to validate the quality of InSAR Envisat/ERS2 phase observations. This validation has been performed using independent precise leveling observations. The estimated precision of the InSAR phase measurements varies, but there is no conclusive evidence that it depends on the viewing geometry. The estimated average precision of the InSAR phase measurements is 4.2 mm (vertical) for ERS2 and 3.4 mm for Envisat.

INTRODUCTION

The persistent scatterer approach in radar interferometry (InSAR) has recently produced spectacular results in the monitoring of deformation processes, [1]. The key points of the persistent scatterer approach are (1) the identification of time-coherent point targets and (2) the systematic decomposition of the atmospheric, topographic, deformation, and residual components of phase observations.

One of the significant problems of the persistent scatterers technique is the association of the quality standards to deformation measurements. An estimate on the quality of the deformation measurement so far has been only based on assumptions on the deformation model and there is a need for independent quality description of InSAR phase (deformation) observations. In this paper we discuss the implications of the systematic decomposition of the phase observations to the deformation, in terms of quality description of the phase measurements, using a controlled corner reflector experiment.

For this reason, since March 2003, Envisat and ERS2 acquisitions from two adjacent descending tracks have been acquired over a test site in Delft, see Fig. 1. Five corner reflectors were deployed and during every satellite acquisition these reflectors have been leveled with millimeter precision. The main objective of the Delft corner reflector experiment is to simulate a set of stable scatterers whose phase history can be validated by additional measurements. A period of more then one year was analyzed in order to gather enough statistics to draw conclusions on the quality of the phase time histories.

Originally developed for the external calibration of the SAR systems, [2], [3], corner reflectors have been successfully applied in the various SAR experiments [4], [5], [6], [7], [8]. With this contribution we extend the application of the corner reflectors to the persistent scatterer analysis.

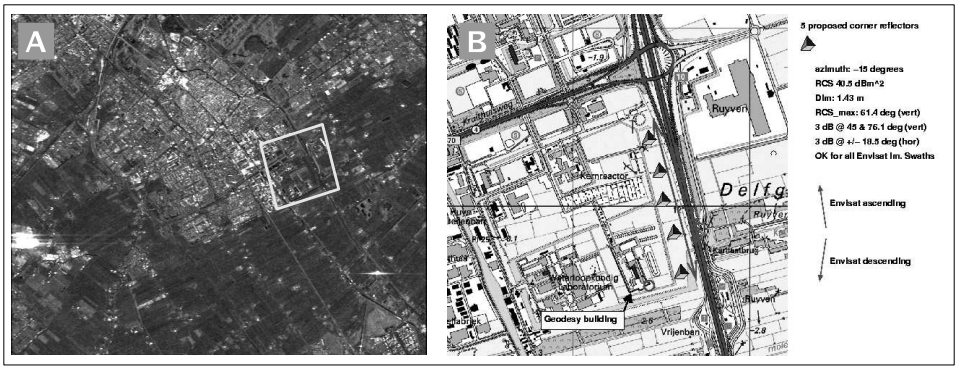

Figure 1: (A) A multi-image reflectivity map of the city of Delft and the corner reflector area. (B) Topographic map of the corner reflector area and details of the radar cross section of the reflectors.

DELFT TEST SITE

Two data sets were independently analyzed, namely two stacks of ERS2 and Envisat data. Both stacks consisted of all available images for the corner reflectors area since the beginning of the experiment (01.03.2003), which sum up in 10 images for ERS2 and 8 for Envisat stack. Additionally, precise orbits for ERS2, acquisitions after 01.09.2003, were computed internally at DEOS. The outline of the data sets and a graphical presentation of their geometrical characteristics are presented in Fig. 2(A).

In Fig. 2(A), all acquisitions are plotted as a function of their spatial and temporal baseline, with respect to a suitable reference image or master. In this case, both the Envisat and ERS2 acquisitions on 10/9/2003 were used as reference. Note that the absolute baseline shift between the ERS2 and the Envisat stack is not implemented - both sets should be interpreted separately.

InSAR Data Processing

Both data sets were processed by DORIS software [9] and [10]. Furthermore, additional scripts for the processing automatization and visualization were developed. The processing was performed in the 'classical way' and the flowchart given by Fig. 2(B) depicts basic processing steps. Resulted interferograms for both stacks are visualized by Fig. 3.

The noisy appearance of ERS2 interferograms, Fig. 3, is due to the large difference in Doppler centroid frequencies ($\Delta\ f_{DC}$). Decorrelation of Envisat, Fig. 3, interferograms is mainly due to the temporal and perpendicular baseline, Fig. 2(A).

Phase Extraction

In order to obtain an estimate of the corner reflector's peak phase at a sub-pixel level the following procedure is used. Firstly, the area of interest, approximately 256x256 complex pixels, is 'cropped' from the interferogram. Secondly, the crop is harmonically interpolated by the factor of 16. Finally, an algorithm for the automatic phase extraction of the reflector, based on the Canny edge detection algorithm, [11], is applied to the interpolated crop.

The following sections provide more details on the complex interpolation and the automatic phase extraction of the corner reflector.

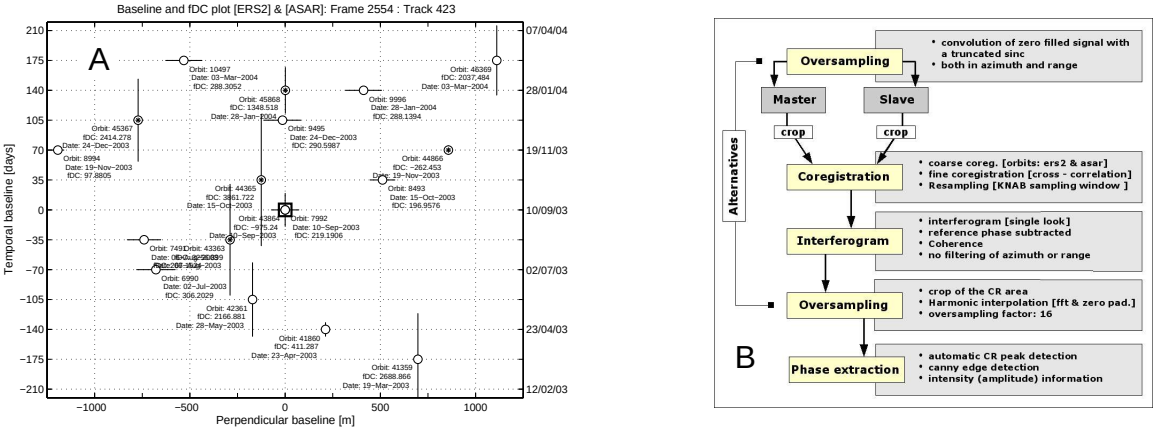

Figure 2: (A) A baseline plot showing information on the temporal and spatial baselines of the ERS2 stack and Envisat stack of acquisitions. Both datasets should be interpreted independently. Doppler information is indicated by the lines. (B) Processing flowchart

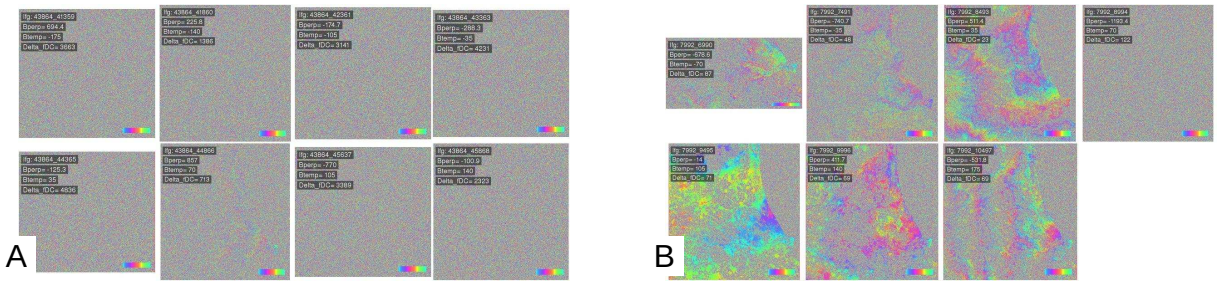

Figure 3: ERS2 (left) and Envisat (right) interferograms (single-master stack) in radar geometry. East is left.

Reconstruction of Phase Signal

The reconstruction of the signal utilizes the fundamental principle that 'zero padding' in one domain results in an increased sampling rate in the other domain [12]. Following this principle, the signal is interpolated by using an FFT and an oversampling factor of 16. The analysis of the phase convergence as a function of the oversampling factor showed that the phase peak becomes 'stable' for an oversampling factor 8.

Automatic Detection of Corner Reflectors

In order to enable an automatic detection of the corner reflectors' peak and localize the sub-pixel position of the reflectors in the interferogram, the Canny edge detection algorithm is adjusted for this particular application. The Canny method finds edges by looking for local maxima of the gradient of the intensity image. The gradient is calculated by using the derivative of a Gaussian filter. The method uses two thresholds, to detect strong and weak edges, and includes the weak edges in the output only if they are connected to strong edges. In this particular case, the value for the lower threshold is set to 0.4 and for the upper threshold 4*(lower threshold) gave the best results. This method is therefore less likely to be 'fooled' by noise than the others (e.g. Sobel, Prewitt, Roberts), and more likely to detect true weak edges. In this way, a reflector's peak is localized and a sub-pixel position is stored as an additional parameter for further analysis.

Phase Contribution by Object Position

The systematic phase offsets, depending on the object position inside the resolution cell (x_{loc}, y_{loc}), were calculated and applied to the detected phases, [13].

$$\Delta\Phi_{azimuth} = \frac{2\pi}{\nu} \cdot x_{loc} \cdot (f_{DC1} - f_{DC2}) = \frac{2\pi}{\nu} \cdot x_{loc} \cdot \Delta f_{DC} \tag{1}$$

$$\Delta\Phi_{range} = \frac{4\pi}{\lambda} \cdot y_{loc} \cdot \left(\sin(\theta_{loc}) - \sin\left(\theta_{loc} + \frac{B_{eff}}{R}\right)\right) \tag{2}$$

These phase contributions are systematic and therefore all interferometric measurements need to be corrected regarding this effect. Since the accuracy of this procedure is limited to a small phase error caused by the object location, a small error will remain if the perpendicular baseline and Doppler centroid frequency difference is high.

There is more of evaluation and deeper analysis and relation of oversampling factor and sub-pixel position with these corrections to be performed.

Ancillary Data - Leveling

For each satellite pass, a leveling of the five corner reflectors has been carried out. Their heights have been determined relative to a well-founded benchmark.

The leveling network has been set up introducing redundant measurements, what makes it possible to detect outliers

and give a quality description of the estimated heights. The leveling measurements are processed applying the Delft adjustment and testing theory, [14] and [15].

A functional model describing the relation between the leveling measurements and the unknown heights is set according to the A-model. For the stochastic model, measurements are considered to be uncorrelated. Hence, the variances corresponding to the five measurements for each sight form the variance-covariance matrix.

It can be concluded, from the analysis, that the precision of the estimated (corner reflectors) heights after the adjustment and testing sequence is around 0.5-1 mm.

Studying the time series of the corner reflector heights with reference to their initial heights, a seasonal effect is visible which appears to be superposed on a secular settling effect of the corner reflectors in the soil. This seasonal effect, which has an amplitude of 1.5-2 cm, corresponds with the monthly temperature changes. Temperature and precipitation information of the area were obtained from the Dutch Meteorological Institute. The initial idea was to vary the heights of the corner reflectors manually in a controlled way. This was done once on the 23/4/2003 for corner reflector 2. However, since the seasonal height variation turned out to be relatively strong, no further deliberate displacements of the corner reflectors have been undertaken. For the InSAR-leveling observations comparison, double differences are calculated with respect to corner reflector 2, Fig. 4(B).

PROCEDURE VALIDATION

In order to be able to compare the InSAR phase observations with the leveling observations, both have to be defined. The leveling heights are referred to the geoid, which is an equipotential surface of the earth gravity field approximated by the mean sea level surface, [16]. InSAR phase observations are wrapped phases along the line of sight of the satellite in a geometric reference frame, [7]. In order to be able to compare the InSAR observations with the leveling observations, following [7], the InSAR observations are converted to mm along the vertical.

There are two possibilities to validate the phase-derived height differences of the corner reflectors, (i) *per interferogram* and (ii) *per corner reflector as a function of time*. The latter is directly comparable to a point stable network, [1]. We start with the results per interferogram, reflecting the double-difference measurements, e.g. height differences relative to the reference (corner reflector 2).

Evaluation per Interferogram in Time

Scatter plots in Fig. 5, with the leveling results on the horizontal axis and the InSAR results on the vertical axis, depicts the basic idea behind the performed analysis. That is the analysis and statistical evaluation of the double-differenced leveling / InSAR height observations with respect to reference point.

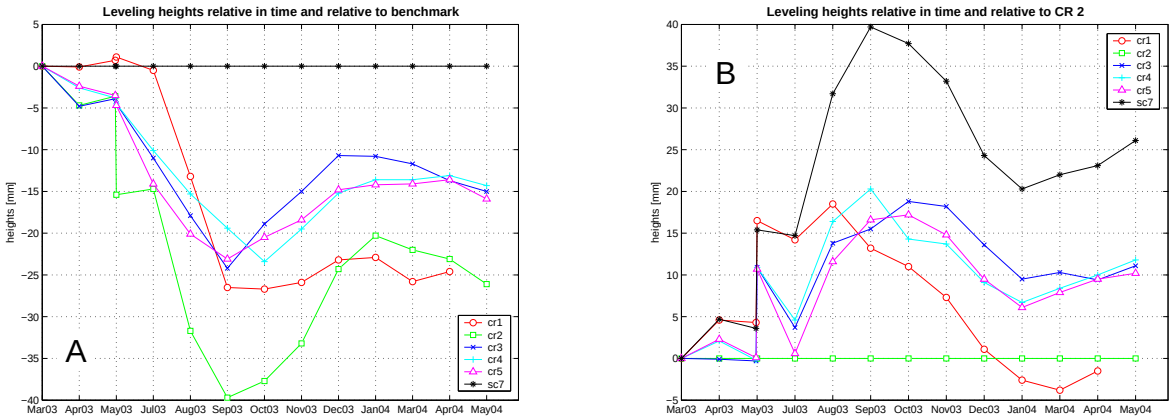

Figure 4: (A) 'Deformation' of the corner reflectors as a function of time, relative to reference point 7. (B) Corner reflector heights relative to CR2, for a direct comparison with the InSAR phase differences.

It is important to note, that since the height datum of the leveling is an arbitrary point, the absolute height differences with respect to the reference point are meaningless. Moreover, since the interferometric phase is also biased by an unknown value, the absolute height differences per reflector in time are meaningless as well. Therefore, similar to a stable point network, [1], double differences of both phase and leveling observations are used for the evaluation.

In the analysis corner reflector 2 is used as a reference and is placed on the $(0, 0)$ coordinate in the each plot. Perfectly identical results would position double differenced observations (of both leveling and InSAR) on the diagonal line. As expected, a certain deviation from the diagonal line is present in all plots.

In order, to assess to what extent the observation and the mathematical model fit, we use an overall model test (OMT or F-test, [15]). In other words, we evaluate the match between the functional model and the stochastic model. In this case, the functional model assume that leveling and InSAR should produce identical results; while the assumption of the stochastic model is that the standard deviation of the phase measurements translates to 4.2 mm standard (double difference) deviation, and that standard deviation of the leveling observation is 1 mm (single height). Using the overall model test we determine which standard deviation we would need in order to accept null-hypothesis. This is decomposed to the single pixel phase-difference standard deviation shown in Fig. 5. Additionally, the offset lines show the estimated model relations, for both ERS2 and Envisat.

The estimates for the formal variance of the InSAR-derived results could be derived from the signal-to-clutter ratio analysis [17], but the variance is here assumed as a constant, indicated by the vertical $1 - \sigma$ error bars on the observations. We used 3 mm standard deviation per phase measurement, [7], which is propagated to standard deviations of phase differences of 4.2 mm. The leveling standard deviation is about 1mm, which is taken into account when evaluating the residues between the phase and the leveling-derived heights.

The variance of the reference point InSAR value is added to the variance of the compared reflectors and the overall model test resulted with a-posteriori variance estimation ($\hat{\sigma}$).

Note that the ambiguity in the InSAR phase observations translates directly to a 30mm ambiguity in the double-difference height. Due to the lack of information on the integer ambiguity value, we simply assume that the results we use for the comparison are the ones which are closest to the leveling ground truth.

In general, figure 5 shows quite good match between the Envisat observations and leveling, whereas the ERS2 data, with a long baseline and/or a very large f_{DC} difference, is not so good. In the case of the Fig. 5(A), the Envisat observations (triangles) match very well to the ground truth of the leveling. On the contrary, Fig. 5(B) shows results of a 70 days interval, which are significantly worse. The results in the Fig. 5(C) are for a period of 105 days; and the maximum deformation of 12mm occurred between the reflectors 2 and 1. For ERS2 (squares), these results are somewhat worse; especially reflectors 3 and 4 deviate significantly from what would be expected. The results in the Fig. 5(C) are poorer probably due to the large perpendicular baseline for the Envisat combination (1193m). In order to interpret such results,

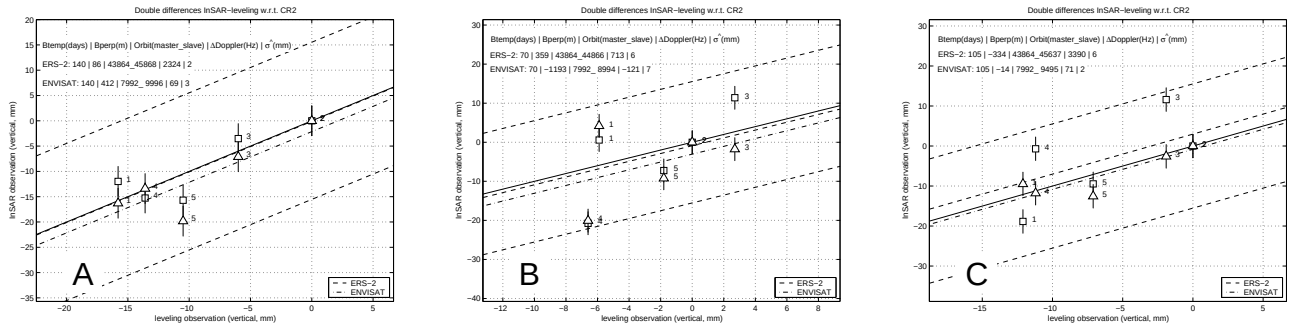

Figure 5: Double-difference height observations with respect to corner reflector 2 as measured by leveling (horizontal axis) and InSAR (vertical axis). The results for the ERS2-ERS2 and Envisat-Envisat interferograms of 10/09/2003 - (A) 19/11/2003, (B) 24/12/2003, and (C) 28/01/2004. ERS2 results are illustrated by dashed line and box, while Envisat with dashed-dot line and triangle.

Table 1: Summary of a-posteriori sigma values of single difference (InSAR) deformation observations

Slave	03/03/03	23/04/03	28/05/03	02/07/03	06/08/03	15/10/03	19/11/03	24/12/03	28/01/04	mean
ERS2	3	3	5	-na-	4	4	6	6	2	4.2
Envisat	-na-	-na-	-na-	6	1	1	7	2	3	3.4

the major characteristics of the interferogram are listed in the figure, which are the perpendicular baseline, the temporal baseline, and the Doppler frequency difference ($\Delta\ f_{DC}$). The latter can be interpreted as an along-track baseline.

The main hypothesis of our analysis is that, in general, the poor results for ERS2 are due to the larger perpendicular baseline and along-track baselines, or better, the change in the viewing geometry between master and slave. If this hypothesis were not be rejected by analysis of several other examples, it could be argued that the assumption, that point scatterers are not (or less) influenced by large changes in viewing geometry, is challenged. We will discuss the effect of changes in viewing geometry on the phase variance later on.

As for the example in Fig. 5(C) the a-posteriori sigma of the ERS2 observations is 6 mm, while the one of Envisat is 2 mm. This implies that we overestimated the quality of the ERS2 observations, whereas the a priori estimate of the Envisat observations was correct.

Generally, it can be concluded that the match between the interferometric results and the leveling supports the hypothesis that radar interferometry is sensitive to the double-difference height variations of an ideal point scatterer such as a corner reflector, although the noise level is quite high in some cases. The a-posteriori sigma values of single difference (InSAR) deformation observations for ERS2 and Envisat are summarized in Table 3. A low a-posteriori sigma value implies a good fit between the leveling and InSAR results.

In overall, the Envisat data is closer to the expected values than the ERS2 data. Although there are different considerations regarding the quality of the physical reflectors, the fact that those dates at which an Envisat interferogram covers exactly the same period as the ERS2 one, up to the shift of 30 minutes, practically rules out the possibility of physical changes in the reflector or its surroundings. Potential causes for the observed differences are therefore the perpendicular and along-track baseline and the noise level of the two radar instruments.

Evaluation per Reflector in Time

The other alternative to evaluate the interferometric observations is to look at the time evolution of a single reflector relative to another. Figures 6(A) and 6(B) show an example of this analysis. The plots show the 'deformation' history of reflector 4 and 5, relative to reflector 2. The bold solid black line connects the leveling values, the dashed line the ERS2 values, and the dash-dot line the Envisat values. The time span covered is more than one year.

It is interesting to note on Fig. 6(A) that the main anomaly, at +70 days is apparent in both, the ERS2 and the Envisat series. Furthermore, the both radar values are actually close together. One possibility for such a systematic difference with the leveling might be a thermal effect of the reflector. The slave date is 19 November 2003, which was not an extremely warm or cold day. Nevertheless, a seasonal signal is visible in both time series.

In the case of the time series of reflector 5 relative to 2, Fig. 6(B), both ERS2 and Envisat show a very nice match with the deformation as observed by leveling, although there seems to be a systematic effect here. The seasonal trend is captured very well though.

Influence of Viewing Geometry

As indicated in the previous sections, it is important to further elaborate on the influence of the significant changes in the viewing geometry on the accuracy or bias of the phase observations. Ideally, for a point scatterer, and especially for a corner reflector, the observed expectation value should be equal for a wide range of perpendicular or along-track baselines.

In order to investigate this relation, Fig. 7(A) and Fig. 7(B) show the observed variability of the InSAR observations around their expected values based on leveling. The variability, expressed as estimated standard deviation, is plotted as a

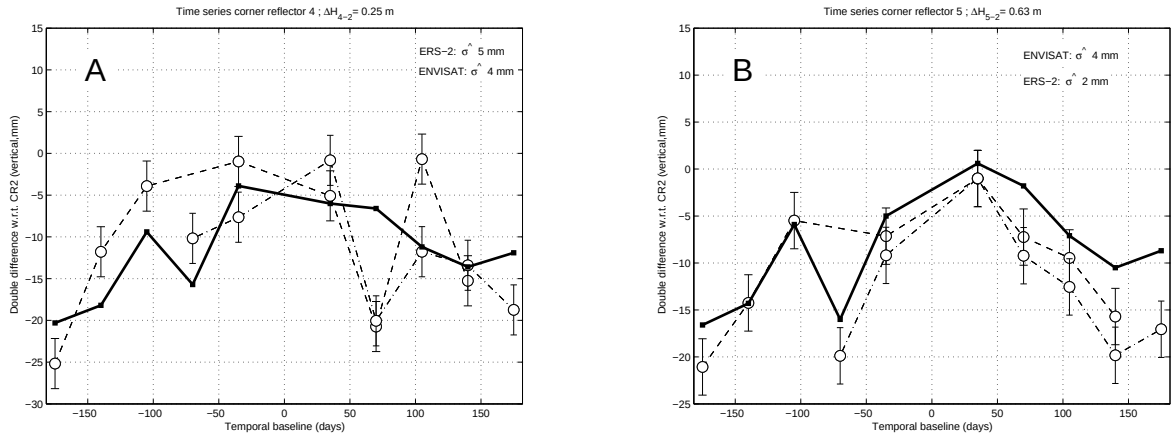

Figure 6: (A) Time series of reflector 4 relative to 2. (B) Time series of reflector 5 relative to 2. Note that the spike in the leveling data (temporal baseline -70) corresponds with the deliberate displacement of cr2. ERS2 results are illustrated by dashed line, while Envisat with dashed-dot line.

function of the along-track baseline (Doppler centroid frequency difference) between acquisitions and their perpendicular baseline.

Fig. 7(A), shows that the hypothesis, that phase variability is related to the viewing geometry (as expected e.g. for distributed scattering), is difficult to prove, since for both situations acquisitions can be found and therefore contradict this hypothesis. With Fig. 7(B) it could be argued that there is a correlation between baseline length (along-track) and perpendicular. However, more extreme values for ERS2 data lead to different conclusions.

Although there is a rank defect which prevents assigning a particular high value of variability to either along-track or across-track baseline, the figures give a rather diffused image. On one hand, the Envisat results suggest correlation between baseline and phase noise, on the other hand, ERS2 results suggest the contrary. Since there are probably more factors involved potentially responsible for an increase in phase noise, such as the not perfect perpendicular orientation of the corner reflector sides, these results cannot confirm the suggestion that an increase in baseline yields to a higher phase noise.

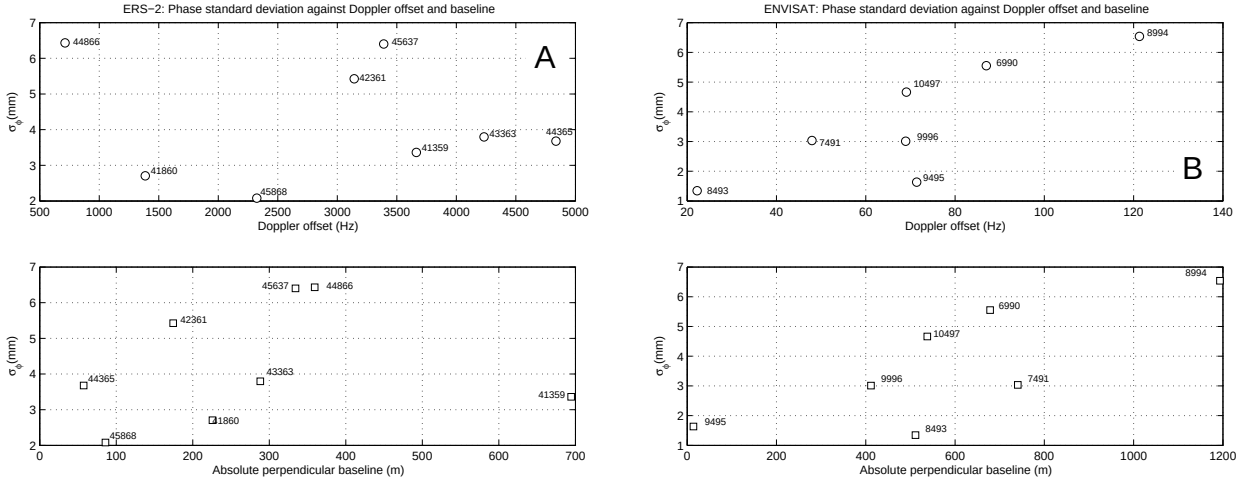

Figure 7: (A) Influence along track or perpendicular baseline on phase quality of ERS2. (B) Influence along-track or perpendicular baseline on phase quality for Envisat.

CONCLUSIONS

The following conclusions could be drawn from the presented study. As expected, persistent scatterers such as corner reflectors are visible in ERS2 and Envisat radar data; and phase continuity for ideal scatterers such as corner reflectors is demonstrated. The phase history comparisons between both sensors in time are comparable in terms that both are able to observe deformation phenomena with a temporal wavelength of about one year. However, particularly for deformation phenomena with a shorter temporal wavelength, there is quite some discrepancy between the two independent data sets. Furthermore, the estimated precision of the InSAR phase single differences is 4.2 mm for ERS2 and 3.4 mm for Envisat, with the assumption that the leveling hight precision is 1 mm. Finally, thirteen experiments over a period of more than one year do not provide conclusive evidence that large perpendicular baselines or large differences in Doppler centroid frequency increase the variance of the phase observations in an unambiguous way.

REFERENCES

[1] A. Ferretti, C. Prati, and F. Rocca. Permanent scatterers in SAR interferometry. *IEEE Transactions on Geoscience and Remote Sensing*, vol. 38, 5:2202–2212, September 2000.

[2] L.M. Ulander. Accuracy of Using Point Targets for SAR Calibration. *IAE*, 27:139–148, 1991.

[3] J.J. Mohr and S.N. Madsen Geometric Calibration of ERS Satellite SAR Images. *IEEE Transactions on Geoscience and Remote Sensing*, vol. 39, 4:842-850, April 2001.

[4] C. Prati, F. Rocca, and A. Monti Guarnieri. SAR interferometry experiments with ERS-1. In *First ERS-1 Symposium–Space at the Service of our Environment, Cannes, France, 4-6 November 1992*, ESA SP-359, pages t 211–217, March 1993.

[5] P. Hartl, M. Reich, K. Thiel, and Y. Xia. SAR interferometry applying ERS-1: some preliminary test results. In *First ERS-1 Symposium–Space at the Service of our Environment, Cannes, France, 4-6 November 1992*, ESA SP-359, pages 219–222, March 1993.

[6] P. Hartl and Y. Xia. Besonderheiten der Datenverarbeitung bei der SAR-Interferometrie. In *Zeitschrift für Photogrammetrie und Fernerkundung*, 6:214–222, 1993.

[7] R. Hanssen *Radar Interferometry: Data Interpretation and Error Analysis*. Kluwer Academic Publishers, 2001.

[8] Y. Xia, H. Kaufmann, and X. Guo Differential SAR Interferometry Using Corner Reflectors. In *International Geoscience and Remote Sensing Symposium, Toronto, Canada, 24-28 June 2002*, cdrom

[9] B. Kampes and S. Usai. Doris: the Delft Object-oriented Radar Interferometric Software. In *2nd International Symposium on Operationalization of Remote Sensing, Enschede, The Netherlands, 16–20 August, 1999*.

[10] B. Kampes, R. Hanssen, and Z. Perski. Public domain tools in radar interferometry. In *Third International Workshop on ERS SAR Interferometry, 'FRINGE03', Frascati, Italy, 3-5 Dec 2003*, pages cdrom, 6 pages, 2003

[11] J. Canny. A Computational Approach to Edge Detection. *IEEE Transactions on Pattern Analysis and Machine Intelligence*, Vol. PAM-8, 6:679–698, 1986.

[12] A.V. Oppenheim, A.S. Willsky, and I.T. Young. *Signals and systems*. Prentice-Hall International, London, 1983.

[13] Altamira. *ENVISAT-ERS exploation: development of algorithms for the explatation of ERS-ENVISAT using the stable points of network*. ESA, Tech. Rep. 16702/02/I-LG, 2004.

[14] P.J.G. Teunissen. *Adjustment theory; an introduction; 1st ed*. Delft: Delft University Press, 2000.

[15] P.J.G. Teunissen. *Testing theory; an introduction; 1st ed*. Delft: Delft University Press, 2000.

[16] P. Vanicek and E.J. Krakiwsky. *Geodesy: the concepts, 2nd edition*. North Holland, Amsterdam, 1986.

[17] N. Adam, B. Kampes, M. Eineder, J. Worawattanamateekul, and M. Kircher. The development of a scientific permanent scatterer system. *ISPRS Workshop High Resolution Mapping from Space, Hannover, Germany, 2003*.